Frequency-stable beamforming over wireless MIMO channels

Christoph F. Mecklenbräuker¹, Peter Gerstoft², Stefan Rotter³, Troels Pedersen⁴

¹Inst. of Telecommunications, TU Wien, Vienna, Austria (ORCID 0000-0001-9571-0379)
²NoiseLab, UC San Diego, La Jolla (CA), USA (ORCID 0000-0002-0471-062X)
³Inst. for Theoretical Physics, TU Wien, Vienna, Austria ORCID 0000-0002-4123-1417
⁴Dept. of Electronic Systems, Aalborg University, Aalborg, Denmark ORCID 0000-0002-3003-4901

ABSTRACT

The Wigner-Smith (WS) matrix provides a powerful framework for characterizing the delay properties of scattering processes in time-invariant propagation environments. When the underlying scattering matrix is unitary, the WS matrix is guaranteed to be Hermitian, with real-valued eigenvalues known as proper delay times. These eigenvalues quantify the delay experienced by narrowband wave packets shaped according to the corresponding WS eigenvectors (also known as "principal modes"). Originally introduced in quantum mechanics to describe collision-induced delays in particle scattering, the WS matrix has since found broader applications. We explore its relevance for wireless multiple-input multipleoutput (MIMO) systems using antenna arrays on both sides of the radio link. In particular, we highlight that the principal modes of the WS matrix exhibit robustness to small frequency shifts, even for the strongly non-unitary scattering matrices commonly encountered in wireless communication scenarios.

I. Introduction

Beamforming under various forms of uncertainty and mismatch has been much investigated, cf. [1]. Here, we demonstrate the usefulness of the Wigner-Smith (WS) matrix for computing a joint transmitter-receiver beamformer which is insensitive to small frequency variations, even in a frequency-selective propagation environment.

The Wigner-Smith (WS) matrix was originally proposed to measure the time-delay in nuclear scattering processes [2], [3], and was later widely employed in electron transport [4] to determine the time an electron spends in a mesoscopic conductor. Any eigenvector of the WS-matrix (or "principal mode") corresponds to an input state with a well-defined group delay (also called "proper delay time") [5], [6], in contrast to states with a large delay spread. Implementing such states experimentally was enabled by wavefront shaping tools such as in acoustics [7], microwave technology [8], [9], and in optics [10], [11].

The interpretation of the real-valued time-delay eigenvalues of the Hermitian WS matrix as proper delay times hinges on the unitarity of the scattering matrix. However, as we show explicitly below, the corresponding eigenvectors, or "principal modes" [5], are insensitive to small shifts in frequency even for non-unitary scattering matrices. Thus, the principal modes

are well-suited as frequency-stable MIMO channel modes for wireless communications and sensing.

II. PROBLEM FORMULATION

Let $\boldsymbol{H}(\omega) \in \mathbb{C}^{N \times M}$ be a general frequency-selective $N \times M$ multiple-input multiple-output (MIMO) transfer function linking M transmit antennas with N receive antennas in the noise-free linear model

$$y(\omega) = H(\omega)x(\omega), \tag{1}$$

where ω is the angular frequency of interest, $\boldsymbol{x}(\omega) \in \mathbb{C}^M$ is the complex-baseband transmit symbol vector and $\boldsymbol{y}(\omega) \in \mathbb{C}^N$ is the corresponding vector of received antenna samples.

In the following, we will demonstrate the benefits of using the $M\times M$ Wigner-Smith (WS) matrix ($^+$ is the pseudo-inverse)

$$Q_{H}(\omega) = -jH^{+}(\omega)\frac{\mathrm{d}H(\omega)}{\mathrm{d}\omega},\tag{2}$$

as transmission of an eigenvector of the WS matrix excites frequency-stable eigenmode propagation.

To show this explicitly, we maximize the received signal power at the single angular frequency ω , subject to a constraint on the tolerated deviation due to a small frequency change,

$$x(\omega) = \arg \max_{x \in \mathbb{C}^M} \|H(\omega)x\|_2^2$$
, (3)

subject to
$$\left\| \frac{\mathrm{d} \boldsymbol{H}(\omega)}{\mathrm{d} \omega} \boldsymbol{x} \right\|_{2}^{2} < \epsilon$$
. (4)

No further constraints are imposed on $x(\omega)$. The corresponding Lagrangian is

$$L(\boldsymbol{x}, \lambda) = \|\boldsymbol{H}(\omega)\boldsymbol{x}\|_{2}^{2} + \lambda \left(\left\| \frac{\mathrm{d}\boldsymbol{H}(\omega)}{\mathrm{d}\omega} \boldsymbol{x} \right\|_{2}^{2} - \epsilon \right)$$
 (5)

with Lagrangian multiplier $\lambda \geq 0$ and we evaluate the KKT conditions [12]. The solution leads to the minimization of the generalized Rayleigh quotient

$$\boldsymbol{x}(\omega) = \arg\min_{\boldsymbol{w} \in \mathbb{C}^{M}} \frac{\boldsymbol{w}^{\mathsf{H}} \left(\frac{\mathrm{d}\boldsymbol{H}(\omega)}{\mathrm{d}\omega}\right)^{\mathsf{H}} \left(\frac{\mathrm{d}\boldsymbol{H}(\omega)}{\mathrm{d}\omega}\right) \boldsymbol{w}}{\boldsymbol{w}^{\mathsf{H}} \boldsymbol{H}^{\mathsf{H}}(\omega) \boldsymbol{H}(\omega) \boldsymbol{w}}, \quad (6)$$

where $(\cdot)^H$ denotes Hermitian transpose

III. FREQUENCY-STABLE PRINCIPLE MODES

The solution to (3)-(4) gives frequency-stable transmit symbol vectors $\boldsymbol{x}(\omega)$, i.e., transmit symbol vectors whose receiverside shape is insensitive to small frequency changes, i.e.,

$$H(\omega)x(\omega) = \eta(\omega)H(\omega + d\omega)x(\omega),$$
 (7)

where $\eta(\omega) \in \mathbb{C}$ is a scalar.

Let the transfer function $H(\omega)$ be modeled by a tapped delay-line model, i.e.,

$$\boldsymbol{H}(\omega) = \sum_{k=0}^{\infty} \boldsymbol{H}_k \mathrm{e}^{-j\omega\tau_k}$$
 (8)

with matrix coefficients $\boldsymbol{H}_k \in \mathbb{C}^{N \times M}$ and positive propagation delays $0 < \tau_0 \leq \tau_1 \leq \dots$ Continuing from (7) gives

$$\boldsymbol{H}(\omega)\boldsymbol{x}(\omega) = \eta(\omega)\sum_{k=0}^{\infty}\boldsymbol{H}_{k}e^{-j\omega\tau_{k}}e^{-j\tau_{k}d\omega}\boldsymbol{x}(\omega)$$
(9)

$$\boldsymbol{H}(\omega)\boldsymbol{x}(\omega) = \eta(\omega)\sum_{k=0}^{\infty}\boldsymbol{H}_{k}e^{-j\omega\tau_{k}}(1-j\tau_{k}d\omega)\boldsymbol{x}(\omega)$$

$$\boldsymbol{H}(\omega)\boldsymbol{x}(\omega) = \eta(\omega)\left(\boldsymbol{H}(\omega) - j\mathrm{d}\omega\sum_{k=0}^{\infty}\boldsymbol{H}_{k}\tau_{k}\mathrm{e}^{-j\omega\tau_{k}}\right)\boldsymbol{x}(\omega)$$

$$\boldsymbol{H}(\omega)\boldsymbol{x}(\omega) = \left(\frac{\eta(\omega)d\omega}{1 - \eta(\omega)}\right) \frac{d\boldsymbol{H}(\omega)}{d\omega} \boldsymbol{x}(\omega)$$
(10)

$$\mathbf{H}(\omega)\mathbf{x}(\omega) = \mu(\omega)\frac{\mathrm{d}\mathbf{H}(\omega)}{\mathrm{d}\omega}\mathbf{x}(\omega) \tag{11}$$

Thus, a frequency-stable transmit symbol vector $\boldsymbol{x}(\omega)$ solves the generalized eigenvector equation (11) with $\mu(\omega) = \frac{\eta(\omega)\mathrm{d}\omega}{1-\eta(\omega)}$. A frequency-stable transmit symbol vector $\boldsymbol{x}(\omega)$ aligns the MIMO channel output vector $\boldsymbol{H}(\omega)\boldsymbol{x}(\omega)$ with $\frac{\mathrm{d}\boldsymbol{H}(\omega)}{\mathrm{d}\omega}\boldsymbol{x}(\omega)$ so these become collinear.

We assume $\boldsymbol{H}(\omega)$ to have full column rank. Then, the left inverse $\boldsymbol{H}^+(\omega)$ exists and equals $\boldsymbol{H}^+(\omega) = (\boldsymbol{H}^{\mathsf{H}}(\omega)\boldsymbol{H}(\omega))^{-1}\boldsymbol{H}^{\mathsf{H}}(\omega)$. Multiplying (11) with $\boldsymbol{H}^+(\omega)$ gives

$$\boldsymbol{x}(\omega) = \mu(\omega)\boldsymbol{H}^{+}(\omega)\frac{\mathrm{d}\boldsymbol{H}(\omega)}{\mathrm{d}\omega}\boldsymbol{x}(\omega).$$
 (12)

Thus, a frequency-stable propagation eigenmode is excited by transmitting an eigenvector of $\mathbf{Q}_{H}(\omega)$ defined in (2) which is known as the WS matrix [2]–[4]. In physics, the WS time-delay matrix is defined in terms of the scattering matrix, rather than the transfer matrix, see the Appendix for a discussion. The prefactor -j in (2) makes $\mathbf{Q}_{H}(\omega)$ Hermitian when $\mathbf{H}(\omega)$ is unitary at ω and small deviations $\omega + \mathrm{d}\omega$.

IV. PROPAGATION GRAPH CHANNEL MODEL

Many analytical wireless MIMO propagation models have been proposed [13], e.g., based on random matrix theory [14], transmit- and receive-side eigenmodes [15], and graph-based models [16]–[18]. In our simulation study, we use the graph-based model shown in Fig. 1 which adequately accounts for both specular and diffuse multipath components in a unified manner. This model is characterized by direct

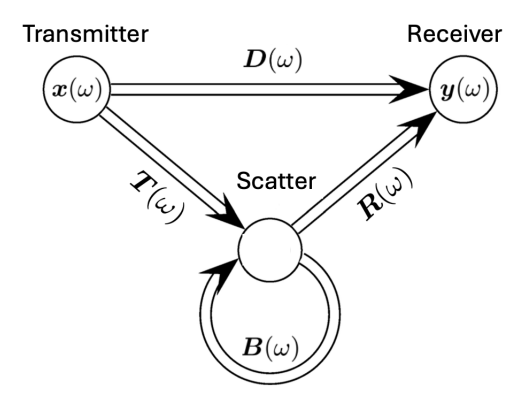


Fig. 1. Propagation graph in a multi-scattering environment.

propagation $D(\omega) \in \mathbb{C}^{N \times M}$ from transmit- to receive-array, propagation from transmit array to S point scatterers $T(\omega) \in \mathbb{C}^{S \times M}$, propagation from S point scatterers to receive array $R(\omega) \in \mathbb{C}^{N \times S}$, and propagation from scatterers to scatterers $B(\omega) \in \mathbb{C}^{S \times S}$, cf. [16, Fig. 3]. The MIMO transfer matrix is

$$H(\omega) = D(\omega) + R(\omega)[I_S + B(\omega) + B^2(\omega) + \dots]T(\omega)$$

= $D(\omega) + R(\omega)(I_S - B(\omega))^{-1}T(\omega)$, (13)

where I_S is the $S \times S$ identity matrix, cf. [17], [18]. This is valid if the spectral radius of $B(\omega)$ is less than 1. All matrix elements represent spherical waves from/to the antennas/scatterers.

V. SIMULATION

We simulate a propagation scenario at $\omega=2\pi\cdot 26\,\mathrm{GHz}$ (corresponding wavelength $\lambda_0\approx 11.53\,\mathrm{mm}$) where the transmitter and the receiver are equipped with uniform circular arrays with N=32 and M=24 antenna elements, respectively, at $0.43\lambda_0\approx 4.96\,\mathrm{mm}$ inter-element spacing under Non-Line-Of-Sight (NLOS) propagation conditions. The wireless link between both antenna arrays is supported by S=10 point scatterers located uniformly at random in a box-shaped volume as shown in Fig. 2. Edges are drawn to connect the transmit array to all scatterers. Furthermore, edges connect scatterers to all scatterers and to the receive array.

We approximate the frequency derivative needed for computing the WS matrix (2) by a finite-difference quotient evaluated at ω and $\omega_1=1.001\omega$. Numerically computed singular values of the corresponding WS matrix $Q_H(\omega)$ are shown in Fig. 3. Note that $Q_H(\omega)$ is non-Hermitian since $H(\omega)$ is not unitary. Therefore, the eigenvalues of $Q_H(\omega)$ differ from the singular values. We observe that S=10 singular values are significant.

Figure 4(top) shows the transmit-side beampattern

$$B_{\mathrm{T}}(\omega, \varphi_{\mathrm{T}}) = 20 \log_{10} \left| \sum_{m=1}^{M} x_m \mathrm{e}^{-j\frac{\omega}{c} \boldsymbol{u}(\varphi_{\mathrm{T}})^{\mathsf{T}} \boldsymbol{r}_{m}} \right|$$
(14)

in the far-field for the selected WS-matrix $Q_H(\omega)$ eigenmode $x(\omega) = (x_1, \ldots, x_M)^\mathsf{T}$ (marked with '*' in red). The transmitside beampattern $B_\mathsf{T}(\omega_1, \varphi_\mathsf{T})$ at the adjacent frequency ω_1

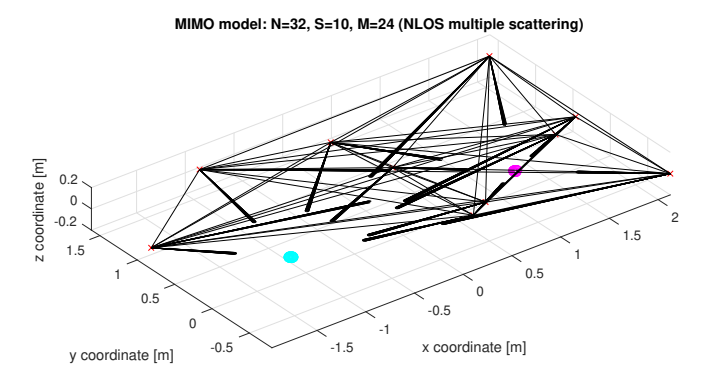


Fig. 2. Simulated propagation scenario: propagation paths (black lines), transmit array (cyan), receive array (magenta), S=10 scatterer locations are marked with 'x' (red).

which uses the same beamformer coefficients x_m (computed at ω) is marginally different (marked with 'o' in blue), but the difference is barely visible in this plot. In (14), $u(\varphi_T)$ is the unit vector oriented towards direction of departure azimuth φ_T , elevation 0, and r_m is the location of the mth transmit antenna element. For comparison, Figure 4(bottom) shows the transmit-side beampattern in the far-field for the (ordinary) eigenmode of $H(\omega)$ (marked with φ in red). Comparing 4(top) with 4(bottom), we observe that these transmit beamformers differ substantially.

Finally, Fig. 5 shows the corresponding receive-side beampatterns

$$B_{\mathrm{R}}(\omega, \varphi_{\mathrm{R}}) = 20 \log_{10} \left| \sum_{n=1}^{N} y_n(\omega) \mathrm{e}^{j\frac{\omega}{c} \boldsymbol{u}(\varphi_{\mathrm{R}})^{\mathsf{T}} \boldsymbol{r}_{n}'} \right|$$
(15)

in the far-field at both frequencies ω and ω_1 where $\boldsymbol{y}(\omega) = \boldsymbol{H}(\omega)\boldsymbol{x}(\omega)$ and $\boldsymbol{y}(\omega_1) = \boldsymbol{H}(\omega_1)\boldsymbol{x}(\omega)$. In (15), $\boldsymbol{u}(\varphi_R)$ is the unit vector oriented towards direction of arrival azimuth φ_R , elevation 0, and \boldsymbol{r}'_n is the location of the nth receive antenna element. Figure 5(top) shows the beampatterns of the WS-matrix eigenmode. The shape of this eigenmode is numerically the same at both frequencies which confirms the desired frequency stability. An important consequence is that the group delay of this mode is precisely defined. Figure 5(bottom) shows the receive-side beampatterns of (ordinary) eigenmode transmission, which changes with frequency and therefore has no frequency stability.

VI. CONCLUSION

The Wigner-Smith (WS) matrix provides a powerful framework for characterizing the delay properties of scattering processes in time-invariant propagation environments. Here, it is demonstrated that the WS-matrix eigenmode serves as a frequency-stable beamformer design. Numerical simulations of a wireless MIMO link in NLOS conditions illustrate the concept.

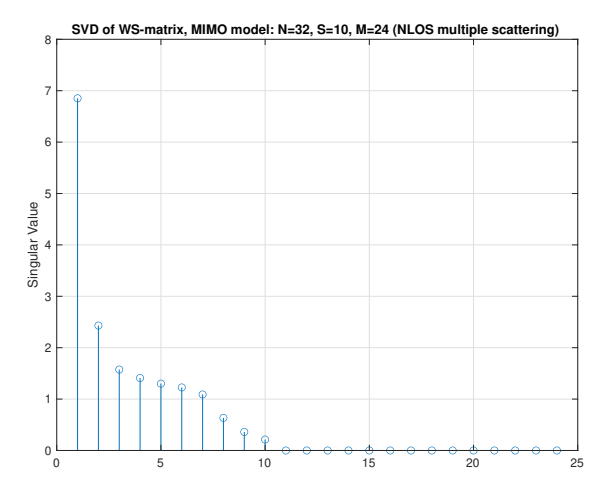
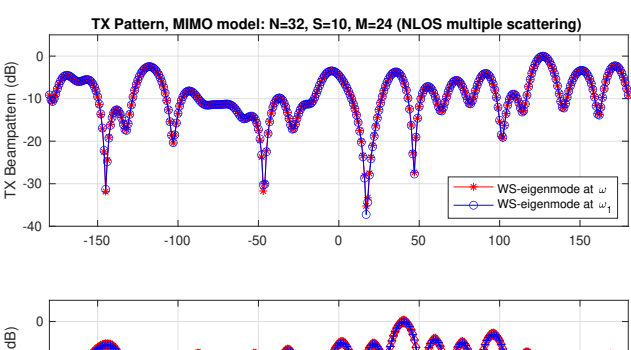


Fig. 3. Singular values of WS matrix ${m Q}_{m H}(\omega)$ for scenario in Fig. 2.



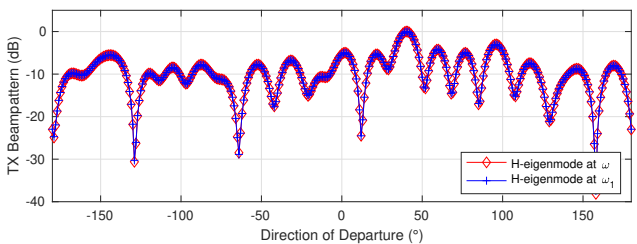


Fig. 4. Transmit beampatterns for scenario in Fig. 2 for WS-eigenmode (top) and H-eigenmode (bottom).

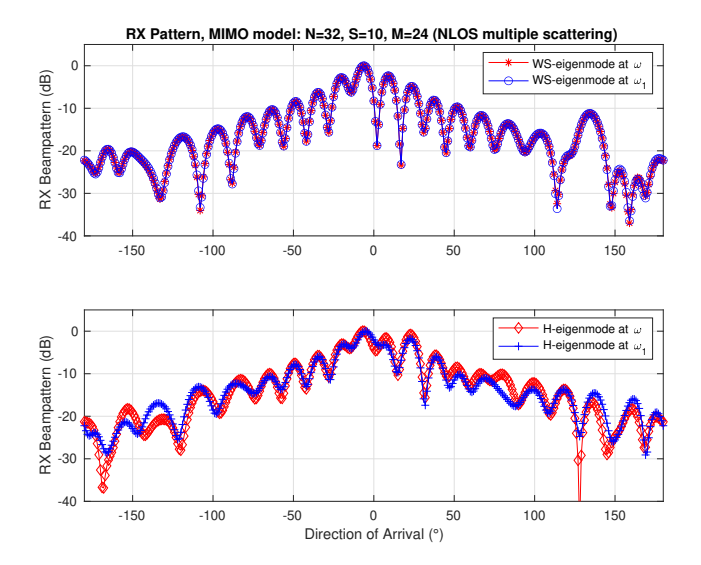


Fig. 5. Receive beampatterns corresponding to transmit beamformers in Fig. 4 for scenario in Fig. 2 for WS-eigenmode (top) and H-eigenmode (bottom).

VII. APPENDIX

In the physics literature, the WS matrix is defined in terms of the scattering matrix $S(\omega)$, i.e.,

$$Q_{S}(\omega) = -jS^{+}(\omega)\frac{\mathrm{d}S(\omega)}{\mathrm{d}\omega}.$$
 (16)

Here, it is shown that $Q_H(\omega)$ defined in (2) is a submatrix of $Q_{\mathbf{S}}(\omega)$ in (16).

The $N \times M$ MIMO transfer function $\boldsymbol{H}(\omega)$ is a sub matrix of the scattering matrix $\boldsymbol{S}(\omega) \in \mathbb{C}^{(M+N)\times (M+N)}$ describing a wireless system with M+N antennas of which M antennas are used for transmission and N for reception. Let $a(\omega)$ and $b(\omega)$ denote the (M+N)-dimensional vectors comprising all incoming and outgoing complex wave amplitudes at the antenna connectors. Assuming linearity, all complex wave amplitudes are related by the noise-free model

$$\boldsymbol{b}(\omega) = \boldsymbol{S}(\omega)\boldsymbol{a}(\omega). \tag{17}$$

It is assumed that reciprocity holds, which guarantees that the scattering matrix is symmetric, $S(\omega) = S^{\mathsf{T}}(\omega)$ where $(\cdot)^{\mathsf{T}}$ denotes matrix transpose. We define

$$\boldsymbol{a}(\omega) = \begin{bmatrix} \boldsymbol{x}(\omega) \\ \mathbf{o}_N \end{bmatrix}, \qquad \boldsymbol{b}(\omega) = \begin{bmatrix} \mathbf{o}_M \\ \boldsymbol{y}(\omega) \end{bmatrix}, \quad (18)$$
$$\boldsymbol{S}(\omega) = \begin{bmatrix} \boldsymbol{\Gamma}_{\mathrm{T}}(\omega) & \boldsymbol{H}^{\mathrm{T}}(\omega) \\ \boldsymbol{H}(\omega) & \boldsymbol{\Gamma}_{\mathrm{R}}(\omega) \end{bmatrix}, \quad (19)$$

$$\mathbf{S}(\omega) = \begin{bmatrix} \mathbf{\Gamma}_{\mathrm{T}}(\omega) & \mathbf{H}^{\mathsf{T}}(\omega) \\ \mathbf{H}(\omega) & \mathbf{\Gamma}_{\mathrm{R}}(\omega) \end{bmatrix}, \tag{19}$$

and o_n is the $n \times 1$ zero vector. Reciprocity requires that $\Gamma_{\rm T}(\omega) = \Gamma_{\rm T}^{\sf T}(\omega)$ and $\Gamma_{\rm R}(\omega) = \Gamma_{\rm R}^{\sf T}(\omega)$. All antenna ports are assumed to be perfectly matched and decoupled at the frequency point ω , giving $\Gamma_{\rm T}(\omega)=\mathbf{0}_M$ and $\Gamma_{\rm R}(\omega)=\mathbf{0}_N$ where $\mathbf{0}_n$ is the $n \times n$ zero matrix. With these definitions, (17) becomes

$$\begin{bmatrix} \mathbf{o}_{M} \\ \mathbf{y}(\omega) \end{bmatrix} = \begin{bmatrix} \mathbf{0}_{M} & \mathbf{H}^{\mathsf{T}}(\omega) \\ \mathbf{H}(\omega) & \mathbf{0}_{N} \end{bmatrix} \begin{bmatrix} \mathbf{x}(\omega) \\ \mathbf{o}_{N} \end{bmatrix}. \tag{20}$$

The second line in (20) equals (1). The pseudo inverse of $S(\omega)$ in (20) is expressible as

$$S^{+}(\omega) = \begin{bmatrix} \mathbf{0}_{M} & H^{+} \\ H^{+\mathsf{T}} & \mathbf{0}_{N} \end{bmatrix}. \tag{21}$$

Therefore,

$$Q_{S}(\omega) = -j \begin{bmatrix} \mathbf{0}_{M} & \mathbf{H}^{+} \\ \mathbf{H}^{+\mathsf{T}} & \mathbf{0}_{N} \end{bmatrix} \frac{\mathrm{d}}{\mathrm{d}\omega} \begin{bmatrix} \mathbf{\Gamma}_{\mathrm{T}}(\omega) & \mathbf{H}^{\mathsf{T}}(\omega) \\ \mathbf{H}(\omega) & \mathbf{\Gamma}_{\mathrm{R}}(\omega) \end{bmatrix}$$
(22)
$$= \begin{bmatrix} \mathbf{Q}_{H}(\omega) & \mathbf{Z}_{\mathrm{R}} \\ \mathbf{Z}_{\mathrm{T}} & \mathbf{Q}_{H^{\mathsf{T}}}(\omega) \end{bmatrix} .$$
(23)

$$= \begin{bmatrix} Q_{H}(\omega) & Z_{R} \\ Z_{T} & Q_{H^{T}}(\omega) \end{bmatrix}.$$
 (23)

where

$$\mathbf{Z}_{\mathrm{R}}(\omega) = \mathbf{H}^{+}(\omega) \,\mathrm{d}\Gamma_{\mathrm{R}}(\omega)/\mathrm{d}\omega$$
 (24)

$$Z_{\rm T}(\omega) = H^{+\mathsf{T}}(\omega) \,\mathrm{d}\Gamma_{\rm T}(\omega)/\mathrm{d}\omega$$
 (25)

Hence, $Q_S(\omega)$ is block diagonal with $Q_H(\omega)$ as a subblock on the main diagonal. In general, the off-diagonal subblocks $\mathbf{Z}_{\mathrm{R}}(\omega)$ and $\mathbf{Z}_{\mathrm{T}}(\omega)$ appearing in (23) are non-zero. Thus, the frequency-stable propagation eigenmode computed as the first M elements of an eigenvector of $\boldsymbol{Q}_{\boldsymbol{S}}(\omega)$ in (16) is different

from the $x(\omega)$ solution in (6). However, the frequency-stability of the beamformer design holds regardless whether $oldsymbol{Z}_{\mathrm{R}}(\omega)$ and $\boldsymbol{Z}_{\mathrm{T}}(\omega)$ are zero matrices or not.

REFERENCES

- [1] H. L. Van Trees, Optimum Array Processing. New York: Wilev-Interscience, 2002, ch. 1-10.
- [2] E. P. Wigner, "Lower Limit for the Energy Derivative of the Scattering Phase Shift," *Physical Review*, vol. 98, no. 1, pp. 145–147, 1955.
- [3] F. T. Smith, "Lifetime Matrix in Collision Theory," Physical Review, vol. 118, no. 1, pp. 349-356, 1960.
- C. Texier, "Wigner time delay and related concepts: Application to transport in coherent conductors," Physica E: Low-dimensional Systems and Nanostructures, vol. 82, pp. 16-33, 2016, frontiers in quantum electronic transport - In memory of Markus Büttiker. [Online]. Available: https://doi.org/10.1016/j.physe.2015.09.041
- S. Fan and J. M. Kahn, "Principal modes in multimode waveguides," Opt. Lett., vol. 30, no. 2, pp. 135-137, Jan 2005. [Online]. Available: https://opg.optica.org/ol/abstract.cfm?URI=ol-30-2-135
- Rotter, P. Ambichl, "Generating and F. Libisch. scattering Phys. Rev. particlelike states in wave transport," vol. 106, p. 120602, Mar 2011. [Online]. Available: https://link.aps.org/doi/10.1103/PhysRevLett.106.120602
- [7] B. Gérardin, J. Laurent, P. Ambichl, C. Prada, S. Rotter, and A. Aubry, "Particlelike wave packets in complex scattering systems," Physical Review B, vol. 94, no. 1, p. 014209, Jul. 2016. [Online]. Available: https://link.aps.org/doi/10.1103/PhysRevB.94.014209
- J. Böhm, A. Brandstötter, P. Ambichl, S. Rotter, and U. Kuhl, "In situ realization of particlelike scattering states in a microwave cavity, Phys. Rev. A, vol. 97, p. 021801, Feb 2018. [Online]. Available: https://link.aps.org/doi/10.1103/PhysRevA.97.021801
- physical Giovannelli and S. M. Anlage, interpretation of imaginary time delay," 2025. [Online]. Available: https://arxiv.org/abs/2412.13139
- [10] J. Carpenter, B. J. Eggleton, and J. Schröder, "Observation of eisenbud-wigner-smith states as principal modes in multimode fibre," Nature Photonics, vol. 9, no. 11, pp. 751-757, Nov 2015. [Online]. Available: https://doi.org/10.1038/nphoton.2015.188
- [11] W. Xiong, P. Ambichl, Y. Bromberg, B. Redding, S. Rotter, and H. Cao, "Spatiotemporal control of light transmission through a multimode fiber with strong mode coupling," *Phys. Rev. Lett.*, vol. 117, p. 053901, Jul 2016. [Online]. Available: https://link.aps.org/doi/10.1103/PhysRevLett.117.053901
- S. Boyd and L. Vandenberghe, Convex Optimization. University Press, 2004.
- [13] P. Almers et al., "Survey of channel and radio propagation models for wireless MIMO systems," EURASIP Journal on Wireless Communications and Networking, vol. 2007, no. 19070, p. 19, 2007. [Online]. Available: https://doi.org/10.1155/2007/19070
- [14] R. R. Müller, "A random matrix model of communication via antenna arrays," IEEE Transactions on Information Theory, vol. 48, no. 9, pp. 2495-2506, 2002.
- [15] W. Weichselberger, M. Herdin, H. Özcelik, and E. Bonek, "A stochastic MIMO channel model with joint correlation of both link ends," IEEE Transactions on Wireless Communications, vol. 5, no. 1, pp. 90-100, 2006. [Online]. Available: https://doi.org/10.1109/TWC.2006.1576533
- T. Pedersen, G. Steinbock, and B. H. Fleury, "Modeling of reverberant radio channels using propagation graphs," *IEEE Transactions on* Antennas and Propagation, vol. 60, no. 12, pp. 5978-5988, Dec. 2012. [Online]. Available: https://doi.org/10.1109/TAP.2012.2214192
- [17] R. Adeogun, A. Bharti, and T. Pedersen, "An iterative transfer matrix computation method for propagation graphs in multiroom environments," IEEE Antennas and Wireless Propagation Letters, vol. 18, no. 4, pp. 616–620, 201 https://doi.org/10.1109/LAWP.2019.2898641 [Online].
- [18] R. Prüller, T. Blazek, S. Pratschner, and M. Rupp, parametrization and statistics of the propagation graphs," 2021 15th European Conference Antennas (EuCAP), 2021, [Online]. pp. https://doi.org/10.23919/EuCAP51087.2021.9410942